ELSEVIER

Journal of Magnetism and Magnetic Materials 218 (2000) 31–41

Journal of magnetism and magnetic materials

www.elsevier.com/locate/jmmm

Magnetic ordering of the $R_6Fe_{13}Sn$ (R = Nd, Pr) compounds studied by neutron diffraction

P. Schobinger-Papamantellos[a,*], K.H.J. Buschow[b], C.H. de Groot[b], F.R. de Boer[b], C. Ritter[c]

[a]*Laboratorium für Kristallographie, ETHZ CH-8092 Zürich, Switzerland*
[b]*Van der Waals-Zeeman Institute, University of Amsterdam Valckenierstr. 65, 1018 XE Amsterdam, Netherlands*
[c]*Institut Laue-Langevin, 156X, 38042 Grenoble Cédex, France*

Received 18 January 2000; received in revised form 3 April 2000

Abstract

The magnetic ordering of $Nd_6Fe_{13}Sn$ and $Pr_6Fe_{13}Sn$ powder samples was investigated by neutron diffraction. The data analysis reveals a collinear antiferromagnetic magnetic moment arrangement of the four Fe and the two R sublattices associated with the wave vector $\boldsymbol{q} = (0\,0\,1)$ corresponding to the I_P magnetic lattice with anticentering translation. The moments of all sublattices located at $(x\,y\,0)$ layers, sandwiched between successive Sn layers perpendicular to z at $z = -0.25, 0.25$ are confined to the same direction. These ferromagnetic blocks change their direction collectively when going to the next Sn layers at $z = 0.25, 0.75$. The structures of the two compounds differ essentially in the preferred direction of antiferromagnetism, which is perpendicular to the c-axis for the $Pr_6Fe_{13}Sn$ compound. For the $Nd_6Fe_{13}Sn$ compound it is along the c-axis for $T > 150$ K and 10° off the c-axis at 1.5 K. The moment values of the R atoms at 1.5 K are 3.06(7) μ_B and 2.45(4) μ_B/Nd atom 2.9(1) μ_B and 2.70(1) μ_B/Pr atom while the average value of the ordered Fe moment is 2.4 μ_B/Fe for both compounds, in satisfactory agreement with Mössbauer results.

Keywords: Magnetic ordering; Neutron diffraction; Antiferromagnetism; Rare earth compounds

1. Introduction

Rare earth compounds of the type $Pr_6Fe_{13}X$ (X = Cu, Ag, Au, Si, Sn, etc.) crystallise in the tetragonal $Nd_6Fe_{13}Si$ structure [1,2] in a space group of 14/mcm. The $R_6Fe_{13}X$ compounds and their magnetic properties are of much interest. They form, in very small amounts, as impurity phases during the sintering of X-doped permanent magnet materials of the type $R_2Fe_{14}B$ where they can act as nucleation centers of domain walls and have a large influence on the coercivity. The structure of the $R_6Fe_{13}X$ compounds is an ordered variant of the $La_6Co_{11}Ga_3$ structure [3] with two rare earth sites R_1 (8f) and R_2 (16l) and four Fe sites Fe_1 (4d), Fe_2 (16k), Fe_3 ($16l_1$) and Fe_4 ($16l_2$). These compounds form only for the first few members of the rare earth series, and their magnetic properties

* Corresponding author. Tel.: +41-1-632-3773; fax: +41-1-632-1133.

E-mail address: schobinger@kristall.erdw.ethz.ch, nelly@kristall.erdw.ethz.ch (P. Schobinger-Papamantellos).

0304-8853/00/$ - see front matter
PII: S0304-8853(00)00351-6

were studied earlier by Weitzer et al. [2]. According to the latter authors the $Nd_6Fe_{13}X$ compounds order magnetically below $T_C = 340\,K$, the magnetic ordering being revealed by a rise of the magnetisation below T_C. Yan et al. [4] and Wang et al. [5] report on the basis of neutron and X-ray data a collinear ferrimagnetic moment arrangement for the $Nd_6Fe_{13}Si$ and $Pr_6Fe_{13}Si$ compounds with the moments forming two antiferromagnetically coupled sublattices: $R_1(8f)\uparrow$, $R_2(16l)\uparrow$, $Fe_1(4d)\uparrow$, $Fe_2(16k)\downarrow$, $Fe_3(16l_1)\downarrow$, $Fe_4(16l_2)\downarrow$, pointing along $\boldsymbol{c}$ as suggested in Ref. [6]. In contrast, neutron diffraction performed by us earlier [7,8] on $Pr_6Fe_{13}Si$ and several other $R_6Fe_{13}X$ compounds with X = Ag or Au revealed collinear antiferromagnetic ordering of the four Fe and of the two R sublattices, associated with the wave vector $\boldsymbol{q} = (0\,0\,1)$. The easy moment direction was found to be perpendicular to the c-direction in all these cases. In the present investigation we have extended our study of the magnetic structure of these compounds to $Nd_6Fe_{13}Sn$ and $Pr_6Fe_{13}Sn$.

Simultaneously we will use this opportunity to correct by a factor of 2 the refined moment value of the Fe1 at 4(d) site given in Refs. [7,8]. This is because the occupation factor used by us was erroneously set to twice its value for the Fe1 site in all refinements of the: $Pr_6Fe_{13}X$ (X = Au, Ag, Si) and $Nd_6Fe_{13}Au$ [7,8] compounds.

2. Sample preparation and magnetic measurements

The $Nd_6Fe_{13}Sn$ and $Pr_6Fe_{13}Sn$ samples were prepared by arc-melting starting materials of at least 99.9% purity. In order to suppress the formation of compounds of the 2:17 type as far as possible we used an excess of about 2% of Nd and Pr. After arc melting the samples were wrapped into Ta foil, sealed into an evacuated quartz tube and annealed for about three weeks at 800°C. After annealing, the samples were quenched to room temperature by breaking the quartz tubes in water.

The X-ray diffraction data showed that the annealed samples of $Pr_6Fe_{13}Sn$ was of single phase, their crystal structure corresponding to the tetragonal $Nd_6Fe_{13}Si$ structure type. In the annealed $Nd_6Fe_{13}Si$ sample, about 5% of an unknown impurity phase was found (see also the neutron diffraction diagrams described in the next section). In order to determine the magnetic ordering temperature of the two compounds investigated we performed magnetic measurements above 300 K on a home-built magnetometer based on the Faraday principle. For these measurements we used polycrystalline lumps in order to avoid oxidation at elevated temperatures as far as possible. The temperature dependence of the magnetization of both the compounds shows a cusp-shaped maxima, similar to those found in other $Nd_6Fe_{13}X$ compounds reported in Ref. [9]. It can be derived from these measurements that both compounds show a Néel type magnetic ordering transition, at $T_N = 393\,K$ for $Pr_6Fe_{13}Sn$ and at $T_N = 433\,K$ for $Nd_6Fe_{13}Sn$.

3. Neutron diffraction

Neutron diffraction experiments were carried out on powder samples of $Pr_6Fe_{13}Sn$ and $Nd_6Fe_{13}Sn$ in the temperature range 1.5–450 K. The data were collected with the high resolution (HR) D1A (double-axis multicounter diffractometers) at the facilities of the ILL in Grenoble using the wavelength of 1.9114 Å in the 0–160° 2θ range. The step increment of the diffraction angle 2θ was 0.1°. The data were corrected for absorption and evaluated by the FullProf Program [10]. Results are shown in Figs. 1–4.

3.1. Nuclear structure of $Pr_6Fe_{13}Sn$ and $Nd_6Fe_{13}Sn$

The neutron diffraction patterns collected in the paramagnetic state at 450 K for $Pr_6Fe_{13}Sn$ and 410 K for $Nd_6Fe_{13}Sn$ are shown in the top parts of Figs. 1 and 3, respectively. The refined parameters given in Tables 1 and 2 confirm the type of structure [1,2]. The R-factor values are satisfactory and indicate no other significant deviation from the basic structure. The strong (0 0 2) nuclear reflection was excluded from the refinements as its peak shape is far from Gaussian due to defects of the neutron optic system of the D1A instrument affecting the low angle range. A small peak shown close to the position of the forbidden (0 0 1) reflection is an artefact due to the beam cutter. As it will be

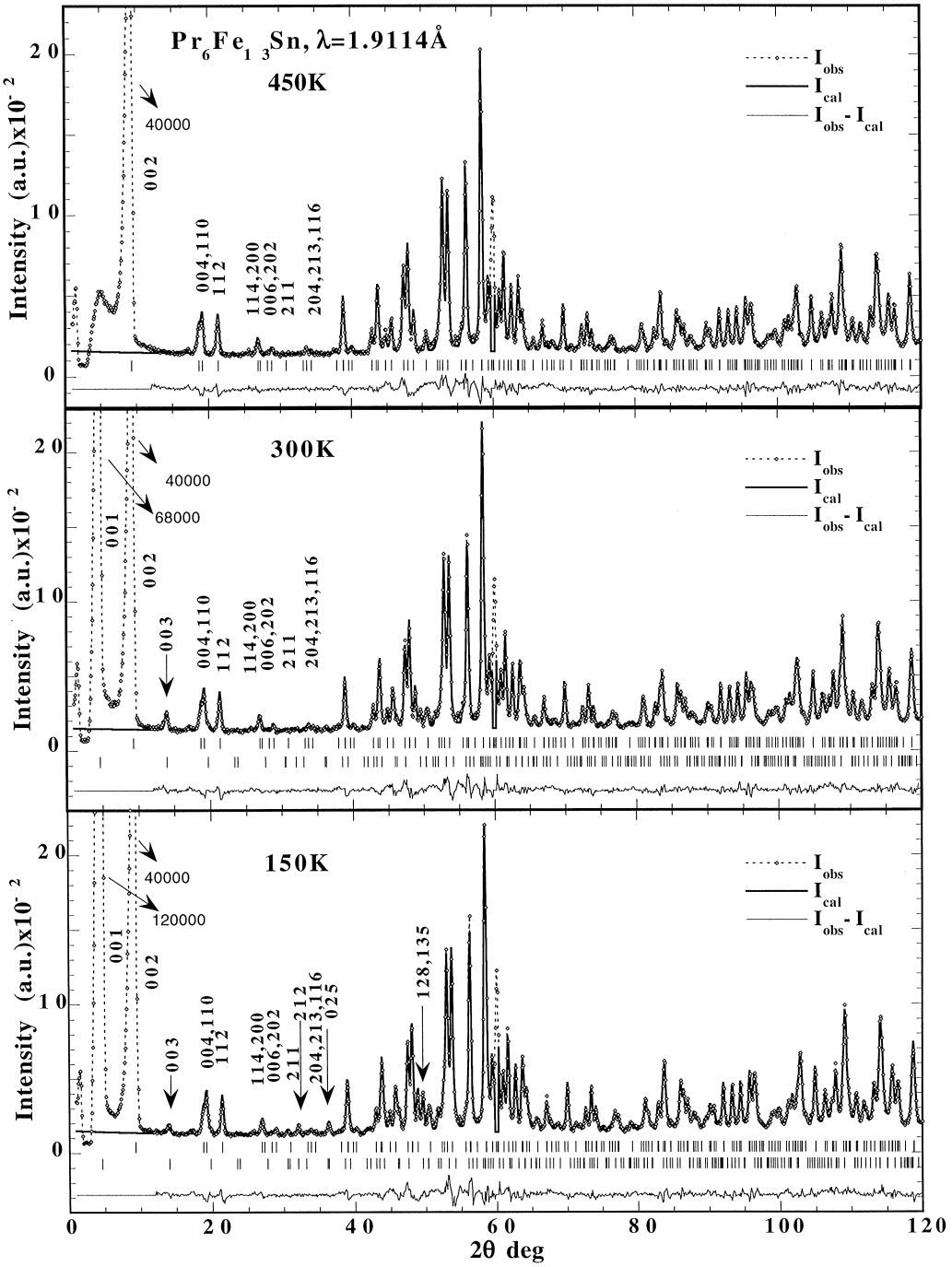

Fig. 1. A part of the observed, calculated and difference neutron HR patterns (D1A diffractometer) of $Pr_6Fe_{13}Sn$ in the paramagnetic state at 420 K and the magnetically ordered state at 300 and 150 K. The strongest magnetic reflections are indicated by arrows.

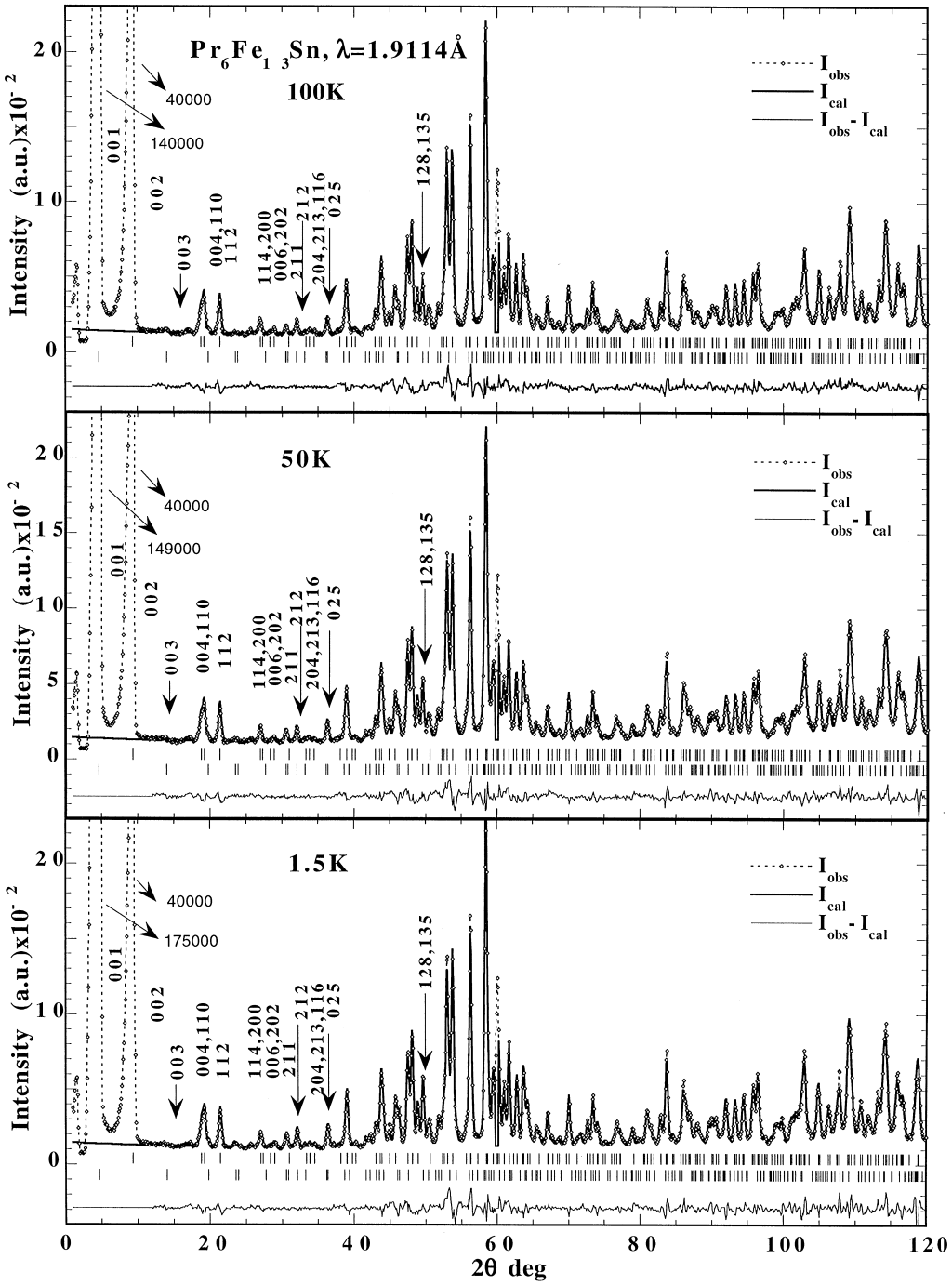

Fig. 2. A part of the observed, calculated and difference neutron HR patterns (D1A diffractometer) of $Pr_6Fe_{13}Sn$ in the magnetically ordered state at 100, 50 and 1.5 K. The strongest magnetic reflections are indicated by arrows.

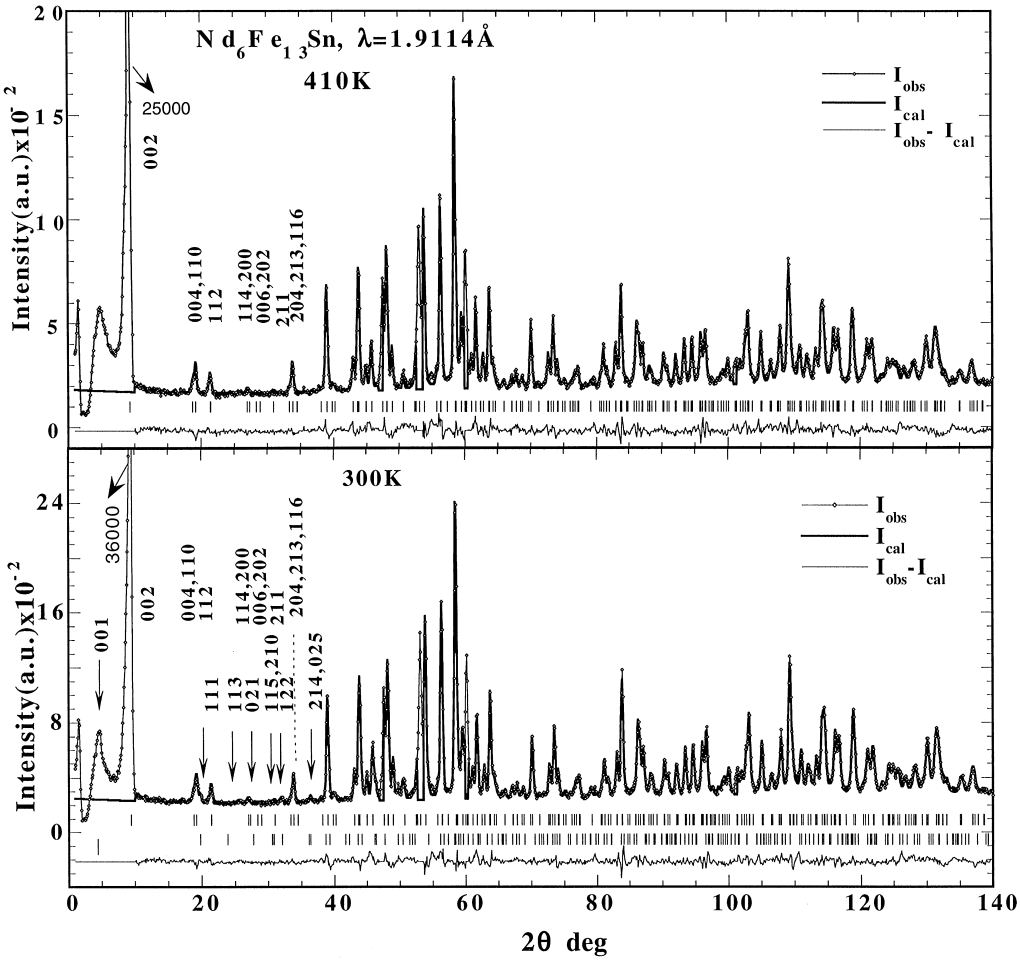

Fig. 3. A part of the observed, calculated and difference neutron HR patterns (D1A diffractometer) of $Nd_6Fe_{13}Sn$ in the paramagnetic state at 420 K and the magnetically ordered state at 300 K. The strongest magnetic reflections are indicated by arrows.

shown below a magnetic contribution to the (0 0 1) reflection may arise below the ordering temperature for a planar moment arrangement.

Alternatively, the choice of a larger wavelength of ≈ 3 Å available for this instrument is not suitable. It would lead to an unfavourable ratio (<4) between the number of refined parameters and the number of independent reflections and hence would not allow a structural refinement. For both samples the peak shape was approximated by a pseudo-voigt function (No. 7 in Ref. [10]) and the background was preferably fitted by a polynomial as the large number of overlapping peaks rendered its graphical estimation difficult. Apparently, in the $Nd_6Fe_{13}Sn$ sample a small amount of an overlapping impurity phase is present that sometimes led to negative temperature factors. The refinement improved while excluding the contributions of a few narrow regions from the refinement.

3.2. Magnetic ordering of $Pr_6Fe_{13}Sn$ ($\boldsymbol{q} = 0, 0, 1$)

The patterns shown in Figs. 1 and 2 for various temperatures in the magnetically ordered state display the same characteristic peak topology with a dominant (0 0 1) reflection at $2\theta = 4.8^\circ$ while all

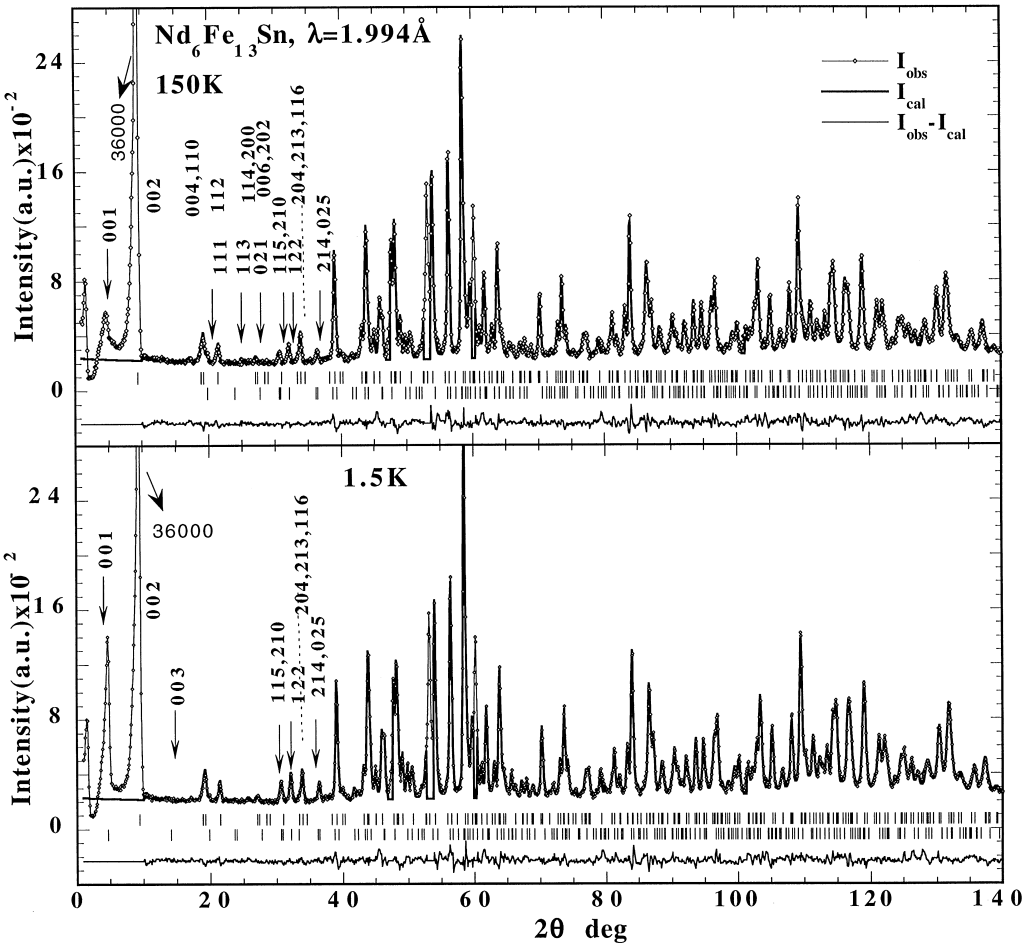

Fig. 4. A part of observed, calculated and difference neutron HR patterns (D1A diffractometer) of $Nd_6Fe_{13}Sn$ in the magnetically ordered state at 150 and 1.5 K. The strongest magnetic reflections are indicated by arrows.

other magnetic contributions are very weak compared with the nuclear reflections even at the lowest temperature. Without the (0 0 1) reflection, the percentage of magnetic intensities does not exceed 12% while including the (0 0 1) reflection it becomes over 40%. However, this reflection was excluded from the refinements for the reasons given above concerning the strong asymmetry of the first nuclear reflection (0 0 2) that cannot be fitted properly.

The presence of odd $(0\,0\,\ell)$ reflections suggests a purely antiferromagnetic structure with the wave vector $\boldsymbol{q} = (0, 0, 1)$. The I-centering condition $(h + k + l = 2n)$ is not fulfilled and the magnetic lattice denoted by I_P [11,12] has a $(\frac{1}{2}, \frac{1}{2}, \frac{1}{2})$ antitranslation. Furthermore, the strong observed (0 0 1) intensity suggests that the preferred axis of antiferromagnetism lies in the (0 0 1) plane. Because of the special position of the Pr1 atom at 8(f) located on the tetragonal $(0\,0\,z)$ axis only uniaxial modes compatible with magnetic space groups comprising a 4_z rotation axis would be allowed. There are four such groups (see Table 3) and only two possible sign sequences are allowed by symmetry for the 8(f) atoms 1: $(0\,0\,z)$; 2: $(0\,0\,\frac{1}{2} - z)$; 3: $(0\,0\,-z)$; 4: $(0\,0\,\frac{1}{2} + z) + I_P$: $(G_z, -G_z)$ $(+\ -\ +\ -\ -\ +\ -\ +)$ and $(A_z, -A_z)$ $(+\ -\ -\ +\ -\ +\ +\ -)$.

Table 1
Refined parameters of $Pr_6Fe_{13}Sn$ (I4/mcm) from (HR, D1A) neutron data in the paramagnetic state at 450 K and the magnetically ordered state at 300, 150, 100, 50 and 1.5 K. μ_{xy} is the refined moment component in the plane (0 0 1)

450 K						300 K				
Atom/site	x	y	z	μ_{xy} (μ_B)	B (nm^2) $\times 10^2$	x	y	z	μ_{xy} (μ_B)	B (nm)$^2 \times 10^2$
Pr1 8f	0	0	0.1039_5	—	2.4_1	0	0	0.1038_4	1.6_1	1.8_1
Pr2 16l	0.1646_6	0.6646_6	0.1859_3	—	2.4_1	0.1641_6	0.6641_6	0.1866_3	0.94_7	1.8_1
Fe1 4d	0.0	0.5	0.0	—	0.97_5	0	0.5	0	2.3_2	0.70_4
Fe2 16k	0.0642_4	0.2087_4	0	—	0.97_5	0.0649_3	0.2100_2	0	1.78_8	0.70_4
Fe3 161_1	0.1791_3	0.6791_3	0.0582_1	—	0.97_5	0.1781_2	0.6781_2	0.0588_1	1.7_1	0.70_4
Fe4 161_2	0.3858_3	0.8858_3	0.0923_1	—	0.97_5	0.3865_2	0.8865_2	0.0933_1	1.7_1	0.70_4
Sn 4a	0.0	0.0	0.25		0.8_2	0	0	0.25		0.11_3
a, c (nm)	0.81024_2	2.3467_1				0.8097_2	2.3483_1			
$R_n, R_m, R_{wp}, R_{exp}$ %	4.2, —, 14, 6					3.3, 12.2, 12.2, 6				
150 K						100 K				
Pr1 8f	0	0	0.1039_3	2.48_9	1.4_1	0	0	0.1043_3	2.71_8	1.4_1
Pr2 161	0.1640_5	0.6640_5	0.1866_2	1.76_5	1.4_1	0.1643_5	0.6643_5	0.1868_2	2.26_5	1.4_1
Fe1 4d	0	0.5	0	2.2_2	0.44_4	0	0.5	0	2.3_2	0.36_4
Fe2 16k	0.0651_3	0.2102_2	0	2.18_6	0.44_4	0.0655_3	0.2103_2	0	2.35_6	0.36_4
Fe3 161_1	0.1783_2	0.6783_2	0.0588_1	2.11_7	0.44_4	0.1784_2	0.6784_2	0.0588_1	2.26_7	0.36_4
Fe4 161_2	0.3867_2	0.8867_2	0.0936_1	2.26_8	0.44_4	0.3867_2	0.8867_2	0.0937_1	2.38_7	0.36_4
Sn 4a	0	0	0.25		0.11_3	0	0	0.25		0.11_4
a, c (nm)	0.8093_2	2.3437_1				0.80919_2	2.3418_1			
R_n, R_m, R_{wp}, R_{exp} %	2.8, 9.7, 12, 5.5					3, 8.8, 12, 5.5				
50 K						1.5 K				
Pr1 8f	0	0	0.1045_4	2.93_8	1.3_1	0	0	0.1044_4	2.91_8	1.0_1
Pr2 16l	0.1648_5	0.6648_5	0.1868_3	2.55_5	1.3_1	0.1644_5	0.6644_5	0.1866_2	2.73_5	1.0_1
Fe1 4d	0	0.5	0	2.2_2	0.30_4	0	0.5	0	2.3_2	0.18_3
Fe2 16k	0.0654_3	0.2104_2	0	2.43_7	0.30_4	0.0655_3	0.2104_2	0	2.57_7	0.18_3
Fe3 161_1	0.1785_2	0.6785_2	0.0588_1	2.45_7	0.30_4	0.1785_2	0.6784_2	0.0588_1	2.42_7	0.18_3
Fe4 161_2	0.3868_2	0.8868_2	0.0937_1	2.51_7	0.30_4	0.3865_2	0.8865_2	0.0937_1	2.54_7	0.18_3
Sn 4a	0	0	0.25		0.16_3	0	0	0.25		0.09_4
a, c (nm)	0.80911_2	2.3406_1				0.80925_2	2.3407_1			
R_n, R_m, R_{wp}, R_{exp} %	2.8, 8, 12, 5.3					2.7, 6.8, 12.8, 5				

However, both modes are incompatible with the experiment as the preferred axis of antiferromagnetism is in the plane. This suggests a symmetry reduction to an orthorhombic or lower space group depending on the absolute moment direction within the plane (0 0 1), as already reported in Ref. [7]. An analysis of the magnetic structure factors of the (0 0 ℓ) reflections of the layered type of structures $R_6Fe_{13}X$ with the wave vector $\boldsymbol{q} = (0, 0, 1)$ was presented in Tables 2 and 3 of Ref. [7]. This analysis led to the development of the model used in the calculations of the $Pr_6Fe_{13}X$, X = Au, Ag, Si and $Nd_6Fe_{13}Au$ compounds [7,8].

The relative intensities of the (0 0 1)/(0 0 3) reflections over the entire magnetically ordered regime display the same behaviour as reported in Refs. [7, 8] for the $Pr_6Fe_{13}Ag$ and $Pr_6Fe_{13}Si$ compounds. The (0 0 3) intensity decreases below 300 K with a gradual increase of the Pr2 moment. This allows using the arguments discussed extensively in Ref. [7], in the numerical analysis of the powder data and favours collinear models with the moments of all sublattices pointing into the same direction within the (0 0 1) plane. The moment arrangement is shown in Fig. 5. The moments of each site are arranged in four successive

Table 2
Refined parameters of $Nd_6Fe_{13}Sn$ (I4/mcm) from (HR, D1A) neutron data in the paramagnetic state at 410 K and the magnetically ordered state at 300, 150 and 1.5 K. μ is the refined moment component and Φ_c its angle with the c-axis

410 K						300 K				
Atom/site	x	y	z	μ (μ_B)	$B(nm^2)\times10^2$	x	Y	z	μ (μ_B) $\Phi_c=0^\circ$	$B(nm^2)\times10^2$
Nd1 8f	0	0	0.1053_3	—	1.4_1	0	0	0.1056_2	1.6_1	0.93_6
Nd2 16l	0.1628_4	0.6628_4	0.1865_2	—	1.4_1	0.1629_3	0.6629_3	0.1866_3	0.99_7	0.93_6
Fe1 4d	0.0	0.5	0.0	—	0.83_6	0	0.5	0	1.8_2	0.56_4
Fe2 16k	0.0654_4	0.2091_4	0	—	0.83_6	0.0664_4	0.2089_4	0	2.0_1	0.56_4
Fe3 161_1	0.1787_3	0.6787_3	0.0588_2	—	0.83_6	0.1785_3	0.6785_3	0.0589_1	1.8_1	0.56_4
Fe4 161_2	0.3866_3	0.8866_3	0.0935_2	—	0.83_6	0.3863_2	0.8863_2	0.0942_1	1.9_1	0.56_4
Sn 4a	0	0	0.25		0.7_2	0	0	0.25		0.493
a,c (nm)	0.8087_8	2.3396_1				0.80877_2	2.3375_1			
R_n, R_n, R_{wp}, R_{exp}%	4.3, —, 14, 8					3.3, 10.6, 12, 6				
150 K				$\Phi_c=0^\circ$		1.5 K			$\Phi_c=10^\circ_3$	
Nd1 8f	0	0	0.1057_2	2.47_8	0.56_6	0	0	0.1059_2	3.06_7	0.20_5
Nd2 16l	0.1629_3	0.6629_3	0.1869_1	1.94_5	0.56_6	0.1633_3	0.6633_6	0.1871_1	2.45_4	0.20_5
Fe1 4d	0	0.5	0	2.2_1	0.32_4	0	0.5	0	2.0_1	0.12_3
Fe2 16k	0.0662_6	0.2089_3	0	2.4_1	0.32_4	0.0663_3	0.2091_3	0	2.67_9	0.12_3
Fe3 161_1	0.1785_2	0.6785_2	0.0591_1	2.2_1	0.32_4	0.1785_2	0.6785_2	0.0589_1	2.45_7	0.12_3
Fe4 161_2	0.3865_2	0.8865_2	0.0945_1	2.32_7	0.32_4	0.3863_2	0.8863_2	0.0946_1	2.53_6	0.12_3
Sn 4a	0	0	0.25		0.04	0	0	0.25		0.08_4
a, c (nm)	0.8083_2	2.3332_1				0.80815_2	2.3298_1			
R_n, R_m, R_{wp}, R_{exp}%	3, 7.9, 11, 5					2.8, 7.8, 11, 5				

Table 3
Possible magnetic space groups of the I4/mcm space group associated with the wave vector $\boldsymbol{q}=(0\,0\,1)$ I_P lattice for the special R position 8(f). Corresponding uniaxial magnetic modes (without $I=\frac{1}{2},\frac{1}{2},\frac{1}{2}$ antitranslation). Column 4 describes the observed (G_x, $-G_x$) and/or (G_y, $-G_y$) modes observed in $Pr_6Fe_{13}Sn$. $Nd_6Fe_{13}Sn$ has a (G_z, $-G_z$) mode compatible with a tetragonal magnetic space group I_P4/mcm (Sh_{124}^{362}) or $I_P4/mc'm'$ (Sh_{127}^{398})

No.	Genel. 8(f)	I4/mcm			Collin model		I_P4/mcm Sh_{124}^{362}	$I_P4/m'c'm'$ Sh_{125}^{374}	$I_P4/mc'm'$ Sh_{127}^{398}	$I_P4/m'cm$ Sh_{130}^{434}
					G_x	G_y	G_z	A_z	G_z	A_z
1	e	0	0	z	+u	+v	— — +w	— — +w	— — +w	— — +w
2	2_y	0	0	$\frac{1}{2}-z$	−u	−v	— — −w	— — −w	— — −w	— — −w
3	i	0	0	$-z$	+u	+v	— — +w	— — −w	— — +w	— — −w
4	c_y	0	0	$z-\frac{1}{2}$	−u	−v	— — −w	— — +w	— — −w	— — +w

ferromagnetic layers at (1): z, (2) $\frac{1}{2}-z$: (4) $\frac{1}{2}+z$; (3): $-z$. coupled antiferromagnetically along $\boldsymbol{c}$ in the sequence (+ − − +). The sign sequence refers to the layers. The moments of the six sublattices form ferromagnetic blocks sandwiched between the X = Sn layers at $z=-0.25$, 0.25, 0.75. The moments change sign collectively when going to the next block.

The refined parameters for six temperatures are summarised in Table 1. The refined moment values f the six sublattices are compared in Fig. 6. Three of the four Fe sites have almost the same average

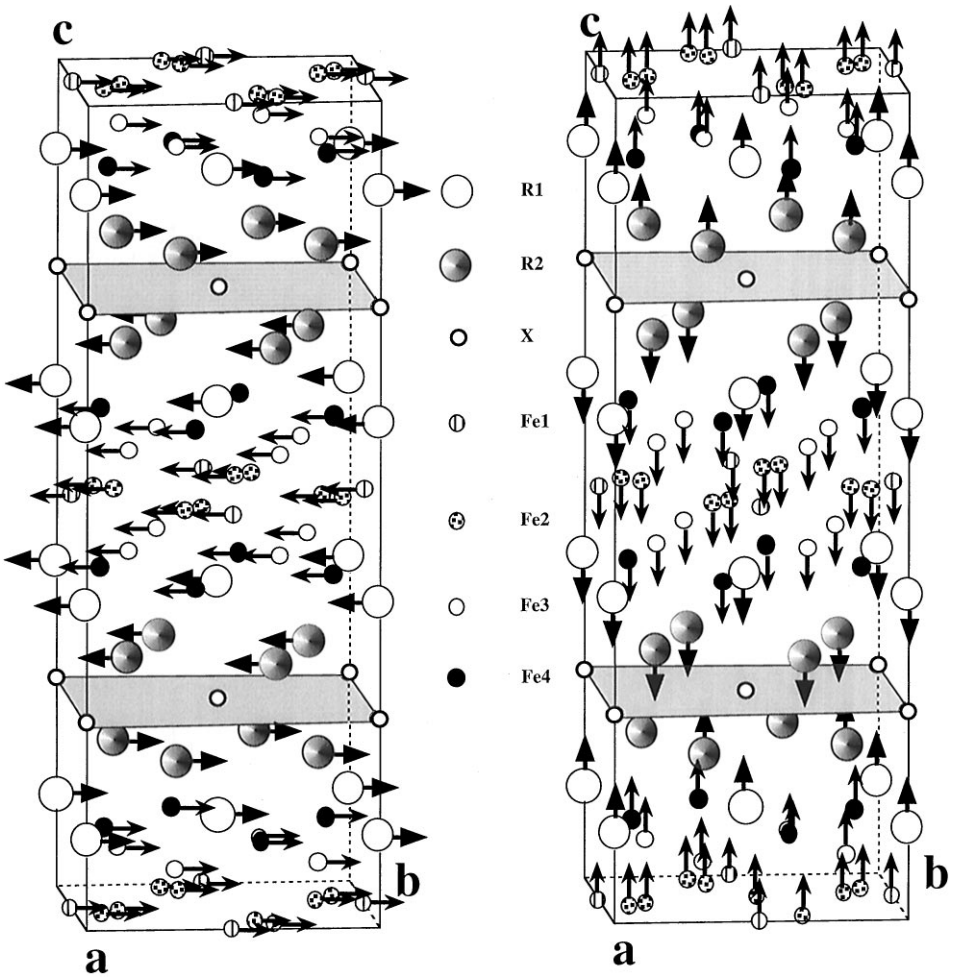

Fig. 5. Schematic representation of the collinear antiferromagnetic structures in $Pr_6Fe_{13}Sn$ (left part) and $Nd_6Fe_{13}Sn$ (right part) with the moments perpendicular to or along the *c*-axis, respectively.

moment value of $2.3_1\ \mu_B$/atom. Excepting the Fe1 site, the other Fe sites behave in a similar manner and reach a saturation moment value of $2.5\,\mu_B$/atom below 100 K. The Fe1 moment behaves quite differently as it achieves a saturation value of $2.3_2\ \mu_B$/atom already at 300 K. The moments of the two Pr sites are equal to $2.9(1)\,\mu_B$ and $2.7(1)\,\mu_B$ at 1.5 K. These values are slightly below the free ion value $gJ\mu_B = 3.2\,\mu_B$, which is most probably due to crystal field effects. The ordering of the two Pr sites seems to proceed in a different way. The Pr1 moments already reach saturation at 50 K while the values of the Pr2 moments are lower by 40–30% between 300 and 150 K, but this difference diminishes at lower temperatures.

3.3. *Magnetic ordering of $Nd_6Fe_{13}Sn$ ($\boldsymbol{q} = 0, 0, 1$)*

Compared to the neutron data of $Pr_6Fe_{13}Sn$, the main feature of $Nd_6Fe_{13}Sn$ patterns collected at various temperatures (see Figs. 3 and 4) in the magnetically ordered regime is the absence of the dominant (0 0 1) reflection at all temperatures. As already said in section 3.1, the peak observed close to the (0 0 1) position for temperatures above 150 K is an artefact from the beam cutter as it also exists

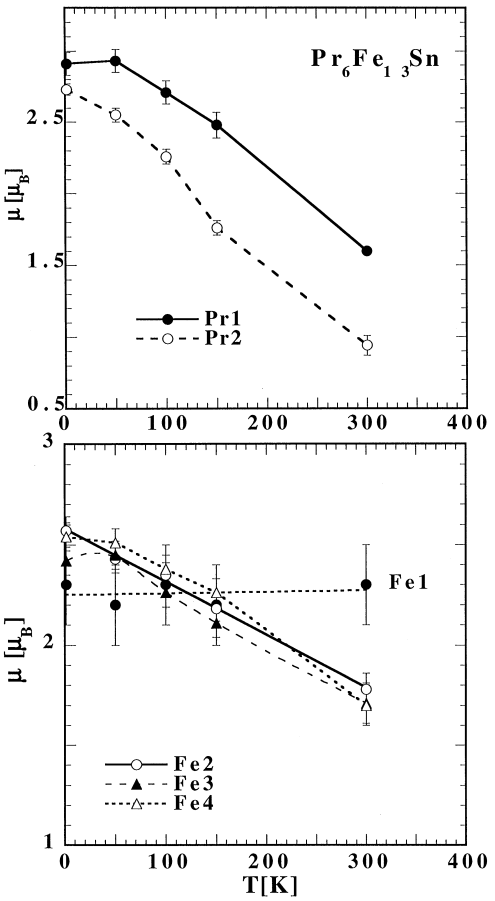

Fig. 6. Thermal variation of the magnetic moments of the Pr and Fe sublattices derived from a limited number of data points below 300 K.

in the paramagnetic state for both examined compounds. A weak reflection at $2\theta = 4.8^\circ$ was only observed in the 1.5 K data. Other magnetic contributions are difficult to distinguish from the nuclear reflections for temperatures above 150 K. This can be seen in the bottom part of Fig. 3, where the strongest magnetic reflections (1 1 5, 2 1 0), (1 2 2) and (2 1 4, 0 2 5) located in the 2θ range 30–40° are almost undistinguishable from the background at 300 K. These reflections do not fullfil the I-centering condition ($h + k + l = 2n$) leading again to the same magnetic lattice I_p with the $(\frac{1}{2}, \frac{1}{2}, \frac{1}{2})$ antitranslation. This suggests a purely antiferromagnetic structure with the wave vector $\boldsymbol{q} = (0, 0, 1)$. Furthermore, the mentioned weak (0 0 1) intensity observed at the lowest temperature suggests that the main axis of antiferromagnetism is confined to the [0 0 1] direction for high temperatures ($T \geqslant 150$) but at a temperature below 150 K, a spin reorientation takes place that gives rise to the intensity of the (0 0 1) reflection at 1.5 K.

The uniaxial magnetic structure realised in $Nd_6Fe_{13}Sn$ does not require symmetry reduction to an orthorhombic phase as for the $Pr_6Fe_{13}Sn$ compound. The possible tetragonal magnetic space groups are I_p4/mcm (Sh^{362}_{124}) or $I_p4/mc'm'$(Sh^{398}_{127}), see also Table 3. The corresponding magnetic structure is displayed in the right part of Fig. 5. The formation of ferromagnetic blocks (out of all six magnetic sublattices) that are coupled antiferromagnetically shows principally the same trend as observed for the $Pr_6Fe_{13}Sn$ compound and the compounds studied in Refs. [7,8]. Only the moment direction is different, being along the *c*-axis for $Nd_6Fe_{13}Sn$.

The agreement factors for the magnetic reflections range between 7 and 12% for all temperatures. This is quite satisfactory if one realises that the magnetic intensity contributions do not exceed 10%. The refined relative moment values of the Nd as well as Fe sublattices show a behaviour similar to that observed for $Pr_6Fe_{13}Sn$. The Fe1 sublattice achieves its saturation value of $2\,\mu_B$/atom already at 300 K. The moments of the other Fe compounds reach the averaged saturation value of $2.5(1)\,\mu_B$/atom below 150 K. Similar to the findings in the $Pr_6Fe_{13}Sn$ compound the moments of the R2 sublattice displays a more damped thermal evolution.

4. Concluding remarks

The magnetic structures of the $Pr_6Fe_{13}Sn$ and $Nd_6Fe_{13}Sn$ compounds are characterised by a ferromagnetic coupling between the 4f moments of the rare earth atoms with the moments of the 3d elements which generally is observed for the light rare earth compounds. The magnetic structures of all isomorphic $R_6Fe_{13}X$ compounds studied by us [7,8], display the same trend of ferromagnetic blocks comprising layers of the six sublattices

which are stacked perpendicular to the c-axis with alternating sign when crossing the X = Si, Ge, Sn, Au, Ag, etc. layers at $z = -0.25, 0.25, 0$. The only difference between the two structures is the uniaxial structure found for the $Nd_6Fe_{13}Sn$ compound. The easy magnetization direction of the latter compound agrees with results of Mössbauer spectroscopy [13]. It is also consistent with a model description proposed in Ref. [14] in which the magnetic anisotropy of several $Nd_6Fe_{13}X$ compounds is taken to depend strongly on the mixing of the Nd valence electron states with the valence electron states of the X atoms, which is very sensitive to the electronic configuration of X. In this model description, the compounds $Nd_6Fe_{13}Au$ and $Nd_6Fe_{13}Sn$ fall into the categories basal plane type anisotropy and uniaxial anisotropy, respectively. This has been confirmed by our neutron experiments.

It was also mentioned in Ref. [14] that the magnetic anisotropy in the $R_6Fe_{13}X$ compounds originates mainly from a crystal field induced R anisotropy in which the second order crystal field parameter carries much weight. The present results show that the situation may be more complicated. For a predominant second-order crystal field parameter one would expect that the $R_6Fe_{13}Sn$ compounds have the same preferred moment direction for R = Pr and Nd because of the same sign of the second-order Stevens factor for the latter two elements. Our neutron diffraction data show, however, that the preferred moment direction is different in these two compounds. Equally important is the fact that we observed a change in $Nd_6Fe_{13}Sn$ from easy axis at high temperatures to easy cone at low temperatures ($\Phi_c \approx 10^\circ$ at 1.5 K). This result suggests that higher-order crystal field parameters also have to be taken into consideration.

We already mentioned that a wrong occupation factor for the 4(d) site of the Fe1 atoms has erroneously been used in two previous investigations [7,8]. The correct occupation factor leads to Fe1 moments twice as high as those listed in Refs. [7,8] for the 4(d) site. After correction, the latter Fe1 moments are in good agreement with those found for $Pr_6Fe_{13}Sn$ and $Nd_6Fe_{13}Sn$ in the course of the present investigation. Also, there is much better agreement with the large hyperfine fields reported in Mössbauer investigations for this Fe site [13,14].

References

[1] J. Allemand, A. Letand, J.M. Moreau, J.P. Nozières, R. Perrier de la Bâthie, J. Less-Common Met. 166 (1990) 73.

[2] F. Weitzer, A. Leithe-Jasper, P. Rogl, K. Hiebl, A. Rainbacher, G. Wiesinger, J. Friedl, F.E. Wagner, J. Appl. Phys. 75 (1994) 7745.

[3] O.M. Sichevich, R.V. Lapunova, A.N. Soboley, Yu.N. Grin, Ya.P. Yarmoluk, Sov. Phys. Crystallogr. 30 (1985) 627.

[4] Q.W. Yan, P.L. Zhang, X.D. Sun, B.P. Hu, Y.Z. Wang, X.L. Rao, G.C. Liu, C. Gou, D.F. Chen, Y.F. Cheng, J. Phys.: Condens. Matter 6 (1994) 3101.

[5] Fangwei Wang, Bao-gen Shen, Huayang Gong, Xiangdong Sun, Panlin Zhang, Qiwei Yan, J. Magn. Magn. Mater. 177–181 (1998) 1056.

[6] Bo-ping Hu, JM.D. Coey, H. Klesnar, P. Rogl, J. Magn. Magn. Mater. 117 (1992) 225.

[7] P. Schobinger-Papamantellos, K.H.J. Buschow, C.H. de Groot, F.R. de Boer, C. Ritter, F. Fauth, Grit Boettger, J. Alloys Comp. 280 (1998) 44.

[8] P. Schobinger-Papamantellos, K.H.J. Buschow, C.H. de Groot, F.R. de Boer, Grit Böttger, C. Ritter, J. Phys.: Condens. Matter 11 (1999) 4469.

[9] C.H. de Groot, F.R. de Boer, K.H.J. Buschow, Dimitri Hautot, Gray J. Long, F. Grandjean, J. Alloys Comp. 233 (1996) 161.

[10] J. Rodríguez-Carvajal, Physica B 192 (1993) 55. (The manual of FullProf can be obtained from a Web browser at http://www-llb.cea.fr/fullweb/powder.htm)

[11] V.A. Koptzik, Shubnikov Groups', Moscow University Print, Moscow, 1966.

[12] W. Opechowski, R. Guccione, in: G.T. Rado, H. Suhl (Eds.), Magnetism IIA, Academic Press, London, 1965, p. 105 Chapter 3.

[13] F. Weitzer, A. Leithe-Jasper, P. Rogl, K. Hiebl, H. Noel, G. Wiesinger, W. Steiner, J. Solid State Chem. 104 (1993) 368.

[14] D. Hautot, G.J. Long, F. Grandjean, C.H. de Groot, K.H.J. Buschow, J. Appl. Phys. 83 (1998) 1554.